

## Electronic Structure and Electron Correlation in $\text{LaFeAsO}_{1-x}\text{F}_x$ and $\text{LaFePO}_{1-x}\text{F}_x$

Walid MALAEB<sup>1\*</sup>, Tepei YOSHIDA<sup>2</sup>, Takashi KATAOKA<sup>1</sup>, Atsushi FUJIMORI<sup>1</sup>, Masato KUBOTA<sup>3</sup>,  
Kanta ONO<sup>3</sup>, Hidetomo USUI<sup>4</sup>, Kazuhiko KUROKI<sup>4</sup>, Ryotaro ARITA<sup>5</sup>, Hideo AOKI<sup>2</sup>,  
Yoichi KAMIHARA<sup>6</sup>, Masahiro HIRANO<sup>6,7</sup>, and Hideo HOSONO<sup>6,7</sup>

<sup>1</sup>*Department of Complexity Science and Engineering and Department of Physics, University of Tokyo, Bunkyo-ku, Tokyo 113-0033*

<sup>2</sup>*Department of Physics, University of Tokyo, Bunkyo-ku, Tokyo 113-0033*

<sup>3</sup>*Institute for Material Structure Science, High Energy Accelerator Research Organization, Tsukuba, Ibaraki 305-0801*

<sup>4</sup>*Department of Applied Physics and Chemistry, The University of Electro-Communications, Chofu, Tokyo 182-8585*

<sup>5</sup>*Department of Applied Physics, University of Tokyo, Bunkyo-ku, Tokyo 113-8561*

<sup>6</sup>*ERATO-SORST, JST, in Frontier Research Center, Tokyo Institute of Technology, Mail Box S2-13, 259 Nagatsuta, Midori-ku, Yokohama 226-8503*

<sup>7</sup>*Frontier Research Center, Tokyo Institute of Technology, Mail Box S2-13, 4259 Nagatsuta, Midori-ku, Yokohama 226-8503*

Photoemission spectroscopy is used to investigate the electronic structure of the newly discovered iron-based superconductors  $\text{LaFeAsO}_{1-x}\text{F}_x$  and  $\text{LaFePO}_{1-x}\text{F}_x$ . Line shapes of the Fe  $2p$  core-level spectra suggest an itinerant character of Fe  $3d$  electrons. The valence-band spectra are generally consistent with band-structure calculations except for the shifts of Fe  $3d$ -derived peaks toward the Fermi level. From spectra taken in the Fe  $3p \rightarrow 3d$  core-absorption region, we have obtained the experimental Fe  $3d$  partial density of states, and explained it in terms of a band-structure calculation with a phenomenological self-energy correction, yielding a mass renormalization factor of  $\sim 2$ .

KEYWORDS: LaFeAsO, electronic structure, photoemission spectroscopy

There is surging interest toward the high- $T_c$  superconductivity recently reported in the iron-based compound  $\text{LaFeAsO}_{1-x}\text{F}_x$ ,<sup>1)</sup> which has been followed by reports on other compounds belonging to the same family,  $\text{LnFeAsO}_{1-x}\text{F}_x$  ( $\text{Ln} = \text{La}, \text{Ce}, \text{Pr}, \text{Nd}, \text{Sm}$ ), with  $T_c$  up to  $\sim 55$  K in  $\text{SmFeAsO}_{1-x}\text{F}_x$ .<sup>2)</sup> The latter  $T_c$  is the highest to date apart from the high- $T_c$  cuprates.  $\text{LaFeAsO}_{1-x}\text{F}_x$  has LaO and FeAs layers alternately stacked along the  $c$ -axis, which renders the compound highly two-dimensional physical properties similar to the cuprates. The parent material LaFeAsO is a semiconductor or a bad metal while the system shows superconductivity with fluorine doping, which is believed to induce electrons into the conducting FeAs layer.<sup>1)</sup>

Although the superconducting gap and pseudogap have been studied by ultra-high resolution photoemission spectroscopy<sup>3-5)</sup> along with a recent report of angle-resolved photoemission spectroscopy (ARPES) on single crystals,<sup>6)</sup> basic knowledge of the electronic structure of the iron-based superconductors that can distinguish themselves from those of other superconductors has yet to come. For example, it is well known that strong electron correlation plays a major role in the high- $T_c$  cuprates, while it is not clear to what extent this applies to  $\text{LaFeAsO}_{1-x}\text{F}_x$ . Also, strong  $p$ - $d$  hybridization exists in the cuprates, whereas no clear idea on this is known for  $\text{LaFeAsO}_{1-x}\text{F}_x$ . Some theoretical works imply

the importance of electron correlations,<sup>7)</sup> and their effects on the unconventional superconductivity.<sup>8-10)</sup> Photoemission spectroscopy (PES) is one of the most powerful tools to study the electronic structure of solids and electron correlation effects. In the present work, we have used PES to investigate the core-level and valence-band spectra of LaFeAsO and LaFePOF.

Polycrystals of  $\text{LaFeAsO}_{1-x}\text{F}_x$  ( $x = 0, 0.06$ ) and  $\text{LaFePO}_{1-x}\text{F}_x$  ( $x = 0.06$ ) were synthesized as described elsewhere.<sup>1,11)</sup> The x-ray photoemission spectroscopy (XPS) measurements were performed using an Mg  $K\alpha$  source ( $h\nu = 1253.6$  eV) at 15 K. The samples were repeatedly scraped with a diamond file to obtain clean surfaces. High-resolution ultraviolet photoemission spectroscopy measurements were performed at beamline 28A of Photon Factory, KEK, with the energy resolution of  $\sim 20$  meV at 15 K. The samples were fractured *in situ* in an ultra-high vacuum below  $1 \times 10^{-10}$  Torr. Theoretical partial density of states has been calculated as follows. We first obtained the band structure in the same way as Kuroki *et al.*<sup>8)</sup> Then, we constructed the maximally localized Wannier functions (MLWFs) for the Fe  $3d$ , As  $4p/P$   $3p$ , and O  $2p$  orbitals using a code developed by Mostofi *et al.*<sup>13)</sup> and calculated Green's function to obtain the spectral function for each MLW.

Figure 1 shows the O  $1s$ , La  $3d$ , As  $3d$  and Fe  $2p$  core-level spectra of LaFeAsO. The single O  $1s$  peak with a largely diminished high-binding energy shoulder

\*malaeb@wyvern.phys.s.u-tokyo.ac.jp

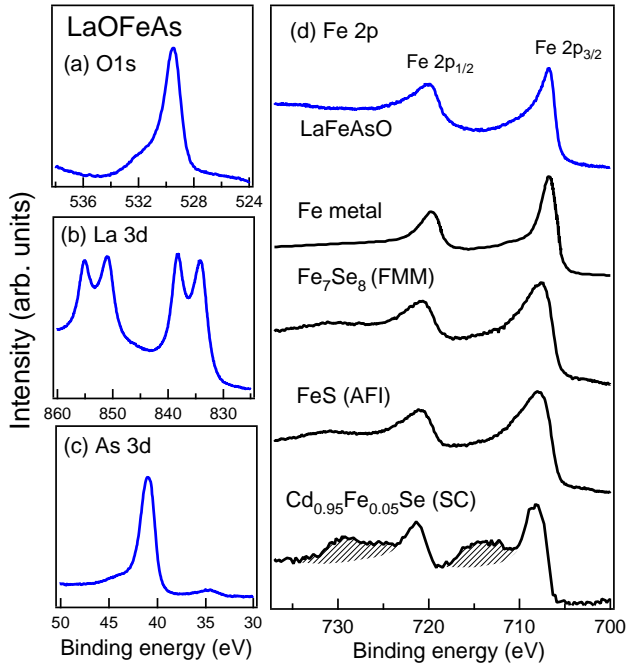


Fig. 1. Core-level XPS spectra of LaFeAsO: (a) O 1s, (b) La 3d, (c) As 3d, (d) Fe 2p. The Fe 2p spectrum is compared with those of Cd<sub>0.95</sub>Fe<sub>0.05</sub>Se (semiconductor), FeS (antiferromagnetic insulator), Fe<sub>7</sub>Se<sub>8</sub> (ferromagnetic metal)<sup>14</sup> and Fe metal.<sup>15</sup>

(Fig. 1(a)) reflects the cleanliness of the sample surface. Nearly identical spectra were obtained for F-doped samples LaFeAsO<sub>0.94</sub>F<sub>0.06</sub> and LaFePO<sub>0.94</sub>F<sub>0.06</sub> (not shown). In Fig. 1(d), the Fe 2p spectrum of LaFeAsO is compared with those of other iron compounds in the literature.<sup>14, 15</sup> The satellites observed in the Fe 2p spectrum of the diluted magnetic semiconductor Cd<sub>0.95</sub>Fe<sub>0.05</sub>Se (shaded area) reflects the localized character of the Fe 3d electrons in this compound.<sup>14</sup> The spectrum of the antiferromagnetic insulator FeS<sup>14</sup> is broad and has a high “background” intensity on the higher binding energy side of the Fe 2p<sub>3/2</sub> peak. On the other hand, the Fe 2p core-level spectrum of LaFeAsO shows no such satellites nor high binding-energy background intensity, while the Fe 2p<sub>3/2</sub> peak itself is as sharp as that of elemental Fe.<sup>15</sup> These observations indicate an itinerant nature of the Fe 3d electrons in LaFeAsO. This is consistent with an NMR result on LaFeAsO, according to which the system shows itinerant antiferromagnetism with  $T_N \sim 142$  K and antiferromagnetic fluctuations in F-doped compounds.<sup>16</sup>

Figure 2 presents the valence-band spectra of LaFeAsO<sub>1-x</sub>F<sub>x</sub> ( $x = 0, 0.06$ ) and LaFePO<sub>0.94</sub>F<sub>0.06</sub>. Main features in the valence band common to the three compounds are a sharp peak near the Fermi level ( $E_F$ ), a weak structure at  $\sim -1.5$  eV, a shoulder at  $\sim -4$  eV and a broad peak at  $\sim -5.5$  eV, consistent with the previous report on LaFeAsO<sub>1-x</sub>F<sub>x</sub>.<sup>3</sup> Similar features are observed

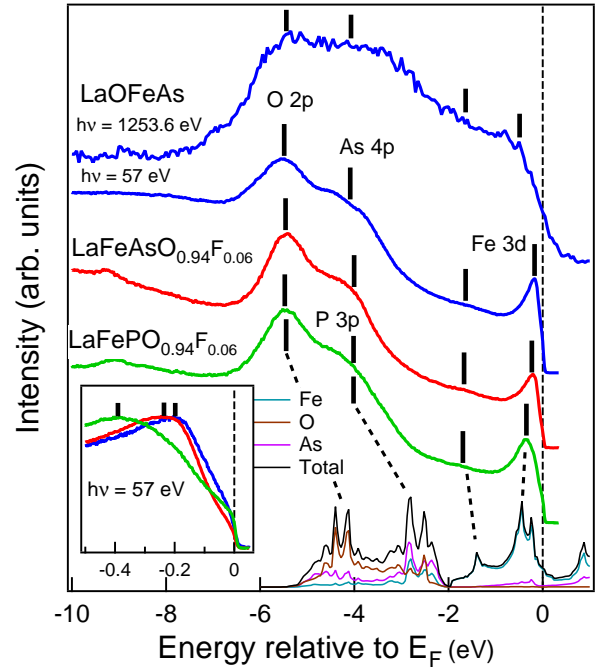


Fig. 2. Valence-band photoemission spectra of LaFeAsO<sub>1-x</sub>F<sub>x</sub> ( $x = 0, 0.06$ ) and LaFePO<sub>0.94</sub>F<sub>0.06</sub> and their comparison with band-structure calculation. Vertical bars mark main features observed in the spectra. The inset presents the near- $E_F$  spectra

in the valence band measured by XPS displayed also in the same figure. For comparison, the band-structure calculation result is displayed at the bottom of Fig. 2. As in the previous calculation,<sup>17</sup> the present result predicts a peak in the density of states (DOS) near the Fermi level, where the main contribution comes from the Fe 3d states. Contributions between -2 and -5 eV are mainly from As 4p/P 3p (at  $\sim -3$  eV) and O 2p (at  $\sim -4.5$  eV). We then attribute the peaks near  $E_F$  in the photoemission spectra to Fe 3d states, while the shoulder around -4 eV and the peak around -5.5 eV to As 4p/P 3p and O 2p states, respectively. Although the experimental data agree qualitatively well with the calculation, some differences are observed where the peak positions near  $E_F$  and the other peaks observed in experiment occur at somewhat lower and higher binding energies, respectively, than predicted by the calculation.

In a blowup near  $E_F$  (inset of Fig. 2), one notices that the peaks are shifted towards higher binding energies with F doping in LaFeAsO<sub>1-x</sub>F<sub>x</sub>. The shift can be explained as a chemical potential shift due to the electron doping. As a result, the intensity of the spectra at  $E_F$  decreases with F doping. Also, the Fe 3d peak for LaFePO<sub>1-x</sub>F<sub>x</sub> is located at higher binding energies and is broad as compared to that of LaFeAsO<sub>0.94</sub>F<sub>0.06</sub>. The broadness of the Fe 3d band of LaFePO<sub>0.94</sub>F<sub>0.06</sub> as com-

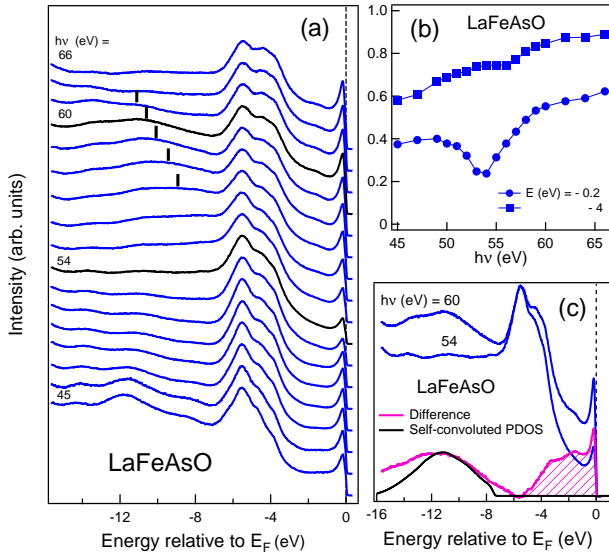


Fig. 3. Valence-band photoemission spectra of LaFeAsO in Fe  $3p \rightarrow 3d$  core absorption region. (a) A series of photoemission spectra for various photon energies. Vertical bars indicate the  $M_{2,3}M_{4,5}M_{4,5}$  Auger peak. (b) Plot of the photoemission intensities at  $E = -0.2$  eV and  $-4.0$  eV as functions of photon energy. (c) Comparison of the self-convolution of the Fe  $3d$  partial density of states (PDOS) (shaded part of the difference spectrum) with the Auger-electron spectrum.

pared to  $\text{LaFeAsO}_{0.94}\text{F}_{0.06}$  has been predicted by band-structure calculations, and can be attributed to the difference in the ionic radii of As and P, which makes the Fe-P distance (0.229 nm) shorter than Fe-As distance (0.241 nm),<sup>1,11)</sup> resulting in a larger value of the hopping parameter ( $t$ ) for LaFePO than that of LaFeAsO. Also, it is noted that  $\text{LaFePO}_{0.94}\text{F}_{0.06}$  has a higher intensity at  $E_F$  than  $\text{LaFeAsO}_{0.94}\text{F}_{0.06}$ . This means that, although  $\text{LaFeAsO}_{0.94}\text{F}_{0.06}$  shows superconductivity at  $T_c \simeq 26$  K, its DOS at  $E_F$  are smaller than those observed for non-superconducting LaFeAsO and  $\text{LaFePO}_{0.94}\text{F}_{0.06}$  with  $T_c = 3$ -5 K. This suggests that effects other than the DOS at  $E_F$ , such as Fermi surface shapes and coupling to boson excitations, may be at work for the superconductivity.

The valence-band spectra of LaFeAsO taken at various photon energies in the Fe  $3p \rightarrow 3d$  core excitation region are shown in Fig. 3(a). Here the spectra have been normalized to the O  $2p$  peak intensity at  $-5.5$  eV. One can see that the intensity of the near- $E_F$  peaks and the  $-4$  eV shoulder show dramatic photon energy dependence: They exhibit an increase from  $h\nu \sim 54$  eV to  $h\nu \sim 60$  eV. The  $h\nu$ -dependence plotted in Fig. 3(b) is indicative of the Fe  $3p \rightarrow 3d$  resonance, and reconfirms that the near- $E_F$  states are mainly Fe  $3d$  states and that the  $-4$  eV shoulder representing the As  $4p$  band is significantly hybridized with Fe  $3d$ .

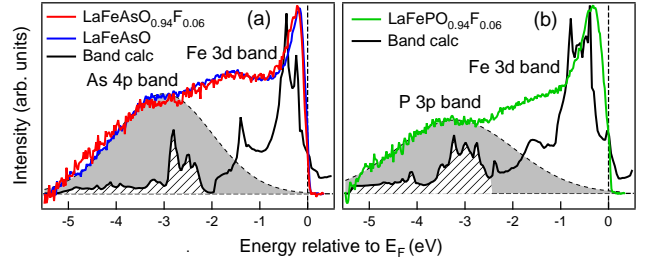


Fig. 4. Fe  $3d$  PDOS of  $\text{LaFeAsO}_{1-x}\text{F}_x$  (a) and  $\text{LaFePO}_{0.94}\text{F}_{0.06}$  (b) determined by subtracting the off-resonance spectra (taken at  $h\nu = 54$  eV) from the on-resonance ones ( $h\nu = 60$  eV) (see Fig. 3(c)). In order to isolate the Fe  $3d$  band, the As  $4p$ /P  $3p$  band assumed to be a Gaussian has been subtracted.

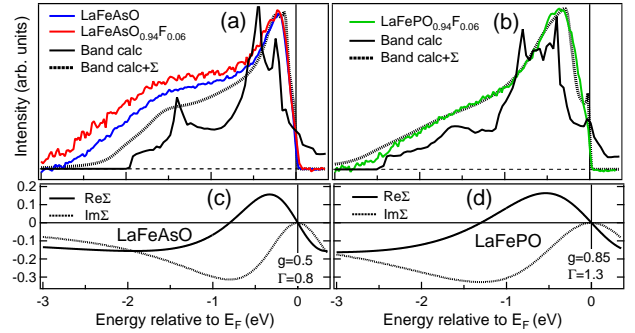


Fig. 5. Results of self-energy corrections to the Fe  $3d$  band for  $\text{LaFeAsO}_{1-x}\text{F}_x$  (a) and  $\text{LaFePO}_{0.94}\text{F}_{0.06}$  (b). (c), (d): Energy dependence of the real and imaginary parts of the empirically determined self-energy  $\Sigma(\omega)$ .

The high binding energy part ( $\sim -6$  eV) of the spectra in Fig. 3(a) also shows a characteristic dependence on photon energy. The broad feature which is shifted to higher binding energies and grows with increasing photon energy, marked by vertical bars in Fig. 3(a), is due to Fe  $M_{2,3}M_{4,5}M_{4,5}$  (Fe  $3p$ - $3d$ - $3d$ ) Auger-electron emission. In the final state of the Auger-electron emission, two holes are left in the Fe  $3d$  band, making Auger electron spectroscopy a good probe to investigate the on-site Coulomb energy.<sup>18)</sup> The good agreement between the Auger spectrum and the self-convolution of the Fe  $3d$  PDOS indicates that  $U \ll 2W$ , where  $U$  is Fe  $3d$  on-site Coulomb energy and  $W$  is the Fe  $3d$  band width,<sup>18)</sup> and therefore most likely  $U < W$ , confirming that the band description of the Fe  $3d$  band is a good starting point to understand the electronic properties of  $\text{LaFeAsO}_{1-x}\text{F}_x$ .

In order to deduce the experimental Fe  $3d$  PDOS, we have subtracted the off-resonance spectra (taken at  $h\nu = 54$  eV) from the on-resonance spectra ( $h\nu = 60$  eV) as shown in Fig. 3(c). The Fe  $3d$  PDOS thus obtained shown in Fig. 4 indicates that the near- $E_F$  peak and the weak peak at  $\sim -1.5$  eV corresponding to Fe  $3d$  bands

survive and that a broad peak corresponding to the As  $4p/P$   $3p$  band appears in the range  $-(3-4)$  eV for every compound. To extract the Fe  $3d$  band, the As  $4p/P$   $3p$  band is approximated by a Gaussian and has been subtracted from the Fe  $3d$  PDOS, leaving the Fe  $3d$ -band part of the Fe  $3d$  PDOS. In order to account for the deviations of the experimental Fe  $3d$  PDOS from the calculated one, we have applied a self-energy correction to the band calculation result. We take an empirical approach, where we assume that electron correlation gives rise to a self energy  $\Sigma(\omega)$ , where  $\Sigma$  is assumed to be  $\omega$ -dependent but momentum independent, to retain the Fermi-liquid properties ( $\Sigma(\omega) \sim -a\omega - ib\omega^2$  in the vicinity of  $E_F$ ) and to satisfy the Kramers-Kronig relation. Here, we take a simple analytical form  $\Sigma(\omega) = -g\omega/(\omega + i\Gamma)^2$ , for which  $\text{Im}\Sigma$  and  $\text{Re}\Sigma$  are shown in Fig. 4(c) and (d), and the parameters are fitted to reproduce the experimental spectra, as has previously done for Fe chalcogenides.<sup>14</sup> While the iron pnictides are theoretically conceived as multiband systems,<sup>8</sup>) this treatment amount to assuming that orbital dependence in the self-energy can be ignored. The single particle spectral DOS,  $\rho(\omega)$ , is thus given by

$$\rho(\omega) = -\frac{1}{\pi} \int d\epsilon N_b(\epsilon) \text{Im} \frac{1}{\omega - \epsilon - \Sigma(\omega)}, \quad (1)$$

where  $N_b(\epsilon)$  is the Fe  $3d$  PDOS given by the band-structure calculation. The  $\rho(\omega)$  thus obtained (Fig. 4(a) and (b)) is seen to exhibit better agreement with experiment. The self-energy gives rise to a mass enhancement,  $m^*/m_b = 1 - \partial \text{Re}\Sigma(\omega)/\partial\omega = 1 + g/\Gamma^2$ , where  $m_b$  is the bare band mass and  $m^*$  the enhanced mass at  $E_F$ . We obtain  $m^*/m_b \simeq 1.8$  for  $\text{LaFeAsO}_{1-x}\text{F}_x$ , and  $m^*/m_b \simeq 1.5$  for  $\text{LaFePO}_{0.94}\text{F}_{0.06}$ . These values are in the same range as the experimental values deduced from the Seebeck coefficient and thermal conductivity.<sup>19</sup>) For more precise discussions, more elaborate analyses of ARPES data with a band-dependent self-energy will be necessary in future studies.

In conclusion, we have investigated the electronic structure of  $\text{LaFeAsO}_{1-x}\text{F}_x$  and  $\text{LaFePO}_{1-x}\text{F}_x$  by photoemission spectroscopy. The Fe  $2p$  core-level spectra indicate an itinerant behavior rather than strongly correlated one. The valence-band spectra are consistent with the band-structure calculations, and show that Fe  $3d$  states are dominant near the Fermi level. Existence of a moderate electron correlation and  $p$ - $d$  hybridization have been demonstrated through the renormalization of the Fe  $3d$  band.

The authors wish to acknowledge Y. Ishida for useful

information on experimental details, and M. Kobayashi for informative discussions. This work was supported by a Grant-in-Aid for Scientific Research in Priority Area ‘‘Invention of Anomalous Quantum Materials’’ from MEXT and by CREST, Japan Science and Technology Agency. W.M. is thankful to MEXT for a financial support. Experiment at Photon Factory was approved by the Photon Factory Program Advisory Committee (Proposal No. 2006S2-001).

- 1) Y. Kamihara, T. Watanabe, M. Hirano, and H. Hosono: J. Am. Chem. Soc. **130** (2008) 3296.
- 2) Z. A. Ren, W. Lu, J. Yang, W. Yi, X. L. Shen, Z. C. Li, G. C. Che, X. L. Dong, L. L. Sun, F. Zhou, and Z. X. Zhao: arXiv:0804.2053.
- 3) T. Sato, S. Souma, K. Nakayama, K. Terashima, K. Sugawara, T. Takahashi, Y. Kamihara, M. Hirano, and H. Hosono: J. Phys. Soc. Jpn. **77** (2008) 063708.
- 4) Y. Ishida, T. Shimojima, K. Ishizaka, T. Kiss, M. Okawa, T. Togashi, S. Watanabe, X.-Y. Wang, C.-T. Chen, Y. Kamihara, M. Hirano, H. Hosono, and S. Shin: arXiv:0805.2647.
- 5) H. Liu, X. Jia, W. Zhang, L. Zhao, J. Meng, G. Liu, X. Dong, G. Wu, R. H. Liu, X. H. Chen, Z. A. Ren, W. Yi, G. C. Che, G. F. Chen, N. L. Wang, G. Wang, Y. Zhou, Y. Zhu, X. Wang, Z. Zhao, Z. Xu, and X. J. Zhou: arXiv:0805.3821.
- 6) C. Liu, T. Kondo, M. E. Tillman, R. Gordon, G. D. Samolyuk, Y. Lee, C. Martin, J. L. McChesney, S. Bud’ko, M. A. Tanatar, E. Rotenberg, P. C. Canfield, R. Prozorov, B. N. Harmon, and A. Kaminski: arXiv: 0806.2147.
- 7) K. Haule, J. H. Shim, and G. Kotliar: Phys. Rev. Lett. **100** (2008) 226402.
- 8) K. Kuroki, S. Onari, R. Arita, H. Usui, Y. Tanaka, H. Kontani, and H. Aoki: arXiv:0803.3325.
- 9) I.I. Mazin, M.D. Johannes, L. Boeri, K. Koepernik, and D.J. Singh: arXiv:0806.1869v1
- 10) X. Dai, Z. Fang, Y. Zhou, and F.-C. Zhang: arXiv:0803.3982.
- 11) Y. Kamihara, H. Hiramatsu, M. Hirano, R. Kawamura, H. Yanagi, T. Kamiya, and H. Hosono: J. Am. Chem. Soc. **128** (2006) 10012.
- 12) I. Souza, N. Marzari and D. Vanderbilt: Phys. Rev. B **65** 035109 (2002).
- 13) A. A. Mostofi *et al.*: <http://www.wannier.org/>.
- 14) K. Shimada, T. Mizokawa, K. Mamiya, T. Saitoh, A. Fujimori, K. Ono, A. Kakizaki, T. Ishii, M. Shirai, and T. Kamimura: Phys. Rev. B **57** (1998) 8845.
- 15) C. D. Wagner, W. M. Riggs, L. E. Davis, J. F. Moulder, and G. E. Muilenberg: Handbook of X-ray Photoelectron Spectroscopy (Perkin-Elmer, Eden, 1979).
- 16) Y. Nakai, K. Ishida, Y. Kamihara, M. Hirano, and H. Hosono: arXiv:0804.4765.
- 17) S. Ishibashi, K. Terakura and H. Hosono: J. Phys. Soc. Jpn. **77** (2008) 053709.
- 18) G.A. Sawatzky: Phys. Rev. Lett. **39** (1977) 504.
- 19) A. S. Sefat, M. A. McGuire, B. C. Sales, R. Jin, J. Y. Howe, and D. Mandrus: arXiv:0803.2528.